A noncontact measurement technique for the specific heat and total hemispherical emissivity of undercooled refractory materials

Aaron J. Rulison[a] and Won-Kyu Rhim
Jet Propulsion Laboratory, California Institute of Technology, 4800 Oak Grove Drive, Pasadena, California 91109

(Received 20 September 1993; accepted for publication 13 December 1993)

A noncontact measurement technique for the constant pressure specific heat (c_{pl}) and the total hemispherical emissivity (ϵ_{Tl}) of undercooled refractory materials is presented. In purely radiative cooling, a simple formula which relates the post-recalescence isotherm duration and the undercooling level to c_{pl} is derived. This technique also allows us to measure ϵ_{Tl} once c_{pl} is known. The experiments were performed using the high-temperature high-vacuum electrostatic levitator at JPL in which 2–3 mm diameter metallic samples can be levitated, melted, and radiatively cooled in vacuum. The averaged specific heats and total hemispherical emissivities of Zr and Ni over the undercooled regions agree well with the results obtained by drop calorimetry: $c_{pl,\mathrm{av}}(\mathrm{Zr})=40.8\pm0.9$ J/mol K, $\epsilon_{Tl,\mathrm{av}}(\mathrm{Zr})=0.28\pm0.01$, $c_{pl,\mathrm{av}}(\mathrm{Ni})=42.6\pm0.8$ J/mol K, and $\epsilon_{Tl,\mathrm{av}}(\mathrm{Ni})=0.16\pm0.01$.

I. INTRODUCTION

The measurements of specific heat of a liquid (c_{pl}) allow us to determine other thermodynamic parameters such as the enthalpy, entropy, and the Gibbs free energy. These quantities measured in the undercooled regions of various materials carry special implications for the studies of solidification processes and for the selection of useful metastable phases.[1,2] However, data on c_{pl} in the undercooled state are relatively scarce because deep undercooling is prohibited by heterogeneous nucleation which is primarily caused by contact with the container walls. In particular, due to their strong chemical reactivity with crucibles, c_{pl} measurements of undercooled states of refractory materials had to wait until adequate containerless processing technologies became available.

There are several approaches one can take to measure c_{pl} of undercooled melts: In drop calorimetry[3,4] a melt undercooled to a known temperature is processed in a levitator, dropped into a calorimeter, and the heat released from the sample is quantified to determine the enthalpy, $H(T)$, as a function of undercooling temperature. $c_{pl}(T)$ is obtained by taking the gradient of $H(T)$ with respect to the temperature and dividing by the sample mass. Although this method is accurate, only one measurement can be made per sample.

In emulsion techniques, undercooling can be achieved by isolating the melts from container walls using appropriate oils which do not catalyze nucleation.[5,6] Differential scanning calorimetry techniques are normally used to measure the heat transfer between the sample (the oil and melt combination) and the calorimeter. Emulsion techniques, however, are only available for relatively low-temperature materials such as Hg, In, Sn, and Bi. Barth *et al.*[7] have recently applied a flux technique to measure c_{pl} of nickel and iron. The use of the post-recalescence isotherm duration to measure the average specific heats of undercooled liquids is similar to the technique described in this paper except that our approach is purely containerless, i.e., no fluxes are required, and it also allows us to measure the total hemispherical emissivity. Further discussions on these points will be given in a later section.

In containerless processing techniques, an undercooled liquid sample is levitated using electromagnetic, acoustic, or electrostatic forces in order to isolate the sample from the container walls. The heat balance of a levitated liquid sample can be expressed by the following equation:

$$m\frac{d}{dt}(c_{pl}T)=-\epsilon_{Tl}\sigma A(T^4-T_s^4)-hA(T-T_s)+Q_{\mathrm{in}}, \quad (1)$$

where m is the sample mass, T is the sample temperature, T_s is the temperature of the surroundings, ϵ_{Tl} is the total hemispherical emissivity, σ is the Stefan–Boltzmann constant, A is the sample's surface area, h is the heat-transfer coefficient which accounts for conductive and convective cooling in a gas, and Q_{in} represents the heat input from external sources. All techniques for measuring c_{pl} of a levitated sample must be based on Eq. (1).

Electromagnetic levitation intrinsically heats the sample at all times unless carried out in low gravity conditions, so, in Earth-based experiments, Q_{in} is non-negligible and must be calculated or measured. Earth-based experiments also require cooling gases to lower the sample temperature. Thus the magnitude of the conductive and convective heat transfer expressed through the coefficient h must be known. These effects combine to make measurement of c_{pl} using electromagnetic levitators in Earth-based laboratories difficult.

Fecht and Johnson[8] have proposed a technique which uses modulation of the heating power in electromagnetic levitation. The necessity, however, of measuring the total hemispherical emissivity ϵ_{Tl} makes the power-modulation approach difficult.

In electrostatic levitation combined with radiant heating, $Q_{\mathrm{in}}=0$ can be achieved in Eq. (1) simply by blocking the heating source. Since the processing environment can

[a]NASA-NRC Resident Research Associate.

 0034-6748/94/65(3)/695/6/$6.00

be high vacuum, the term including h in Eq. (1) can be neglected. Thus the heat balance is purely radiative, and Eq. (1) can be reduced to

$$m\frac{d}{dt}(c_{pl}T) = -\epsilon_{Tl}\sigma A(T^4 - T_s^4). \quad (2)$$

This equation is the basis for the measurements of c_{pl} and ϵ_{Tl} described in this paper.

II. EXPERIMENTAL APPARATUS

The experiments were performed using the high-temperature high-vacuum electrostatic levitator (HTHVESL) at the Jet Propulsion Laboratory.[9] The HTHVESL uses feedback control to position samples between parallel plate electrodes. The sample and electrodes are contained in a stainless-steel vacuum chamber which is typically evacuated to 10^{-7} Torr. Samples 2.5 mm in diameter can be heated to about 2300 K using a focused 1 kW xenon arc lamp. Because electrostatic levitation does not intrinsically transfer heat to the sample, samples can be cooled to room temperature by extinguishing the arc lamp.

Sample radiance is recorded using a single-color optical pyrometer operating at 658 nm (filter width: 10 nm FWHM) and set to 2 kHz bandwidth. The pyrometer views a spot on the sample about 1 mm in diameter. The radiance is converted to temperature using the method described by Hofmeister *et al.*,[10] wherein the spectral emissivity of the sample is assumed to be independent of temperature and equal to the value realized immediately after recalescence. The known melting temperature of the material is used to scale the data according to Planck's equation for the spectral radiance. The data acquisition and analysis are done automatically using a Macintosh-II computer.

III. MEASUREMENT TECHNIQUE FOR SPECIFIC HEAT

The present technique is based on the purely radiative cooling of an isolated spherical sample. Figure 1 shows a typical temperature versus time trace for a 40.0 mg sample of zirconium. The section of the curve before point 1 is unusable because light from the arc lamp reflected from the sample surface into the pyrometer. The proper measurement of sample temperature begins at point 1. The section after point 6 was obtained by blocking the pyrometer and is used for calibration purposes. At $t=0$, the sample had already reached a steady state temperature of 2195 K (67 K above T_m). The sample was spherical and did not show any oscillation. At point 1, a shutter positioned in front of the arc lamp was closed to block the beam completely. In the absence of input energy, the sample cooled radiatively. At point 2, the sample had cooled to T_m. The sample remained liquid and continued to cool below T_m to 1800 K at point 3, at which time solidification started. Thus the sample was in the undercooled state during the time between points 2 and 3. Solidification progressed rapidly and raised the sample's temperature to T_m at point 4 due to recalescence. The sample approximately maintained T_m until point 5, after which its temperature fell again.

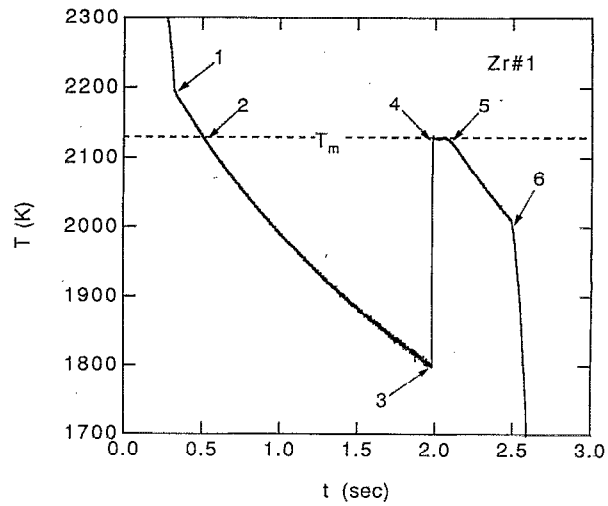

FIG. 1. A typical temperature T vs time t curve for a 40.7 mg zirconium sphere (Zr No. 1) undergoing radiative cooling.

An energy balance can be written for the cooling process which occurred between any two points in the temperature versus time trace, assuming that the sample did not support large temperature gradients in its interior, i.e., the Biot number was small. Consider the balance of energy between points 2 and 5 in Fig. 1. Since the sample was completely molten at point 2, its specific enthalpy here h_2 can be expressed by

$$h_2 = h_f + h_5, \quad (3)$$

where h_f is the specific enthalpy of fusion, and h_5 is the specific enthalpy at point 5 which is given by

$$h_5 = \int_{T_{\text{ref}}}^{T_m} c_{ps}(T)\,dT, \quad (4)$$

where T_{ref} is an arbitrary reference temperature below T_m, and c_{ps} is the specific heat capacity of the solid. If the temperature gradients in the sample are negligible, then the sample can be assumed to be completely solid at point 5. Therefore, the difference in enthalpy between points 2 and 5 is the heat of fusion, h_f, and in the purely radiative cooling, it can be expressed by

$$mh_f = -\int_{T_2}^{T_3} mc_{pl}\,dT + \int_{t_4}^{t_5} \epsilon_{Tm}\sigma A(T_m^4 - T_s^4)\,dt, \quad (5)$$

where ϵ_{Tm} is the total hemispherical emissivity in the isothermal region following recalescence. The heat emitted between points 3 and 4 is negligible because the time spent there is short compared to the time spent between points 2 and 5. Placing constant terms outside the integrals, Eq. (5) can be rewritten as

$$mh_f = m\int_{T_u}^{T_m} c_{pl}\,dT + \sigma(T_m^4 - T_s^4)\int_{t_4}^{t_5} \epsilon_{Tm}A\,dt, \quad (6)$$

where T_2 and T_3 have been replaced by T_m and T_u, which are the melting temperature and the undercooled temperature just before the onset of solidification, respectively. The relationship between T_u, t_4, and t_5 can be measured

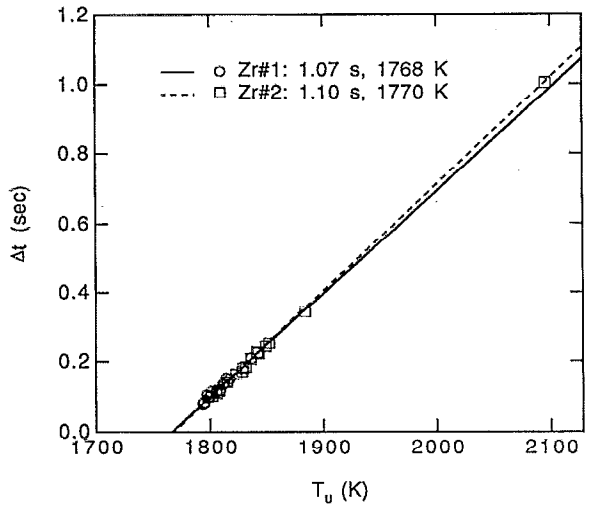

FIG. 2. Post-recalescence isotherm duration, $\Delta t(=t_5-t_4)$, vs undercooling temperature T_u for Zr. No. 1 (40.7 mg) and Zr No. 2 (40.0 mg). Δt_m and T_{hyp} are given in the legend.

experimentally using temperature versus time traces such as Fig. 1. These quantities can then be related to c_{pl} and ϵ_{Tm} using Eq. (6). It is important to note that the total hemispherical emissivity of the undercooled liquid, ϵ_{Tl}, does not appear in Eq. (6), so it need not be measured. Rather, c_{pl} depends on the total hemispherical emissivity at the melting temperature, ϵ_{Tm}. That is, accurate determination of c_{pl} is in general hinged upon detailed knowledge of ϵ_{Tm} which may or may not be available. However, a temperature-averaged c_{pl} can be obtained without any knowledge of ϵ_{Tm}.

Consider the case where t_4 and t_5 are equal, i.e., the post-recalescence isotherm duration is zero. Then Eq. (6) becomes

$$h_f=\int_{T_u}^{T_m} c_{pl}\,dT. \tag{7}$$

In this case T_u is the temperature which marks the onset of hypercooling, T_{hyp}. The intersection of a plot of $\Delta t(=t_5-t_4)$ vs T_u with the abscissa determines T_{hyp} (see Fig. 2). Then, from Eq. (7), the average c_{pl} of the undercooled liquid $c_{pl,\text{av}}$ is given by

$$c_{pl,\text{av}}=\frac{h_f}{T_m-T_{\text{hyp}}}. \tag{8}$$

Thus $c_{pl,\text{av}}$ can be found without having any knowledge of the total hemispherical emissivity of the liquid or the solid. Equation (8) shows that the accuracy of $c_{pl,\text{av}}$ depends directly on the accuracy of h_f, which must be measured by other means.

Now we consider the case where $T_u=T_m$, i.e., the liquid did not undercool. Equation (6) becomes

$$mh_f=\sigma(T_m^4-T_s^4)\int_{t_4}^{t_5} A\epsilon_{Tm}\,dt. \tag{9}$$

Assuming A is constant, Eq. (9) may be used to find an average total hemispherical emissivity, $\epsilon_{Tm,\text{av}}$, for the isotherm region, i.e.,

$$\epsilon_{Tm,\text{av}}=\frac{mh_f}{\sigma(T_m^4-T_s^4)A\Delta t_m}, \tag{10}$$

where Δt_m is determined from the intersection of a plot of $\Delta t(=t_5-t_4)$ vs T_u with the ordinate (see Fig. 2). The sample density in the isotherm region must be known in order to calculate A.

If sufficient data on ϵ_{Tm} is available to solve the second integral on the right-hand side of Eq. (6), then Eq. (6) can be used to calculate the temperature dependence of c_{pl} in the undercooled region. Data on ϵ_{Tm} required to calculate $c_{pl}(T_u)$ include its dependence on T_u as well as its dependence on time after recalescence. Such data were not available for the present study.

Equation (2) shows that $c_{pl}(T_u)$ and $\epsilon_{Tl}(T_u)$ determine the relationship between temperature versus time in the undercooled region. Thus, if either $c_{pl}(T_u)$ or $\epsilon_{Tl}(T_u)$ is known, the other can be calculated from the cooling curve. Although in general the calculation must be made numerically, a simple analytical result can be derived if a plot of time versus T^{-3} results in a straight line, in which case $\epsilon_{Tl}A/c_{pl}$ is constant. Then integration of Eq. (2) gives

$$t_f-t_0=\frac{mc_{pl}}{3\sigma\epsilon_{Tl}A}(T_f^{-3}-T_0^{-3}), \tag{11}$$

where 0 and f refer to any two points in the undercooled region. If $c_{pl,\text{av}}$ and A are known, a straight line fitted to the data plotted as t_f vs T_f^{-3} can be used to determine an average total hemispherical emissivity of the undercooled liquid, $\epsilon_{Tl,\text{av}}$.

Since $c_{pl}(T_u)$ is determined by the distribution of points on the Δt vs T_u plot, the accuracy of $c_{pl}(T_u)$ will improve as the data points are distributed more widely over the temperature range between T_m and T_{hyp}.

IV. EXPERIMENTAL PROCEDURES AND RESULTS

A. Zirconium

Zirconium samples of 99.95% nominal purity were obtained from Teledyne Wah-Chang, Albany, Oregon, and prepared at Vanderbilt University by arc-melting in an argon atmosphere on a water-cooled plate to form them into approximate spheres. Experiments were performed on two zirconium samples, Zr No. 1 and Zr No. 2, whose masses were 40.7 and 40.0 mg, respectively. Plots of Δt vs T_u for both samples are shown in Fig. 2. There was some natural variation of T_u from one undercooling experiment to the next, but the range was quite narrow. Therefore, in order to extend the range of T_u, a preliminary method of triggering nucleation was used. This consisted of bleeding in oxygen to form patches of an oxide layer on the sample's surface. Although successful in triggering nucleation over a wider range of undercooling temperatures than occurred naturally, this method is likely to have altered the total hemispherical emissivity of the sample, and is, therefore, far from ideal. But, the video records show that the surface

area covered by the oxide layer patches was limited to a few percent of the sample's total area, so the results presented below are not affected greatly, although spikes in the radiance measurement were observed when oxide patches moved into the area on the pyrometer viewing area. Other methods for triggering nucleation are under development.

The temperature reading in the post-recalescence isotherm region did not remain exactly constant. For example, in one run it fell 7 K over 0.85 s isotherm duration, which is 0.33% of T_m. This may be due in part to the changing spectral emissivity and in part due to an actual surface temperature variation. If the total hemispherical emissivity changed while the actual surface temperature remained constant, then a 0.33% error would appear in the measured Δt. If the variation in the temperature reading was due to an actual surface temperature change then it must result in slower cooling than assumed. This effect could be reconciled by applying a correction factor which would result in a 1.3% decrease in the measured Δt. Any systematic error in Δt cannot affect $c_{pl,\mathrm{av}}$ appreciably since it would not affect T_{hyp} in Eq. (8), while it can affect $\epsilon_{Tm,\mathrm{av}}$ proportionately through Δt_m in Eq. (10). In this study, however, no such corrections have been applied since the errors in Δt are smaller than the experimental uncertainties associated with h_f and ρ_m.

Δt vs T_u plots are shown in Fig. 2. The data points are well represented by straight lines over the range of undercooling temperatures tested. Since Δt_m and T_{hyp} were not realized experimentally, it seems reasonable to determine them by extrapolating straight line fits to the data. The hypercooling temperatures for Zr No. 1 and Zr No. 2 were determined to be 1768 ± 5 and 1770 ± 2 K, respectively. Using Eq. (8) the values of the average specific heat capacities of the undercooled liquid $c_{pl,\mathrm{av}}$ of Zr No. 1, Zr. No. 2 are determined to be 40.7 ± 0.9 and 40.9 ± 0.9 J/mol K, assuming $h_f=14.652\pm0.32$ kJ/mol.[11] The value of $c_{pl}(T_m)$ determined by Bonnel (1972) using drop calorimetry is 40.7 ± 0.7 J/mol K, which agrees well with the present result for the undercooled liquid. We emphasize that the accuracy of $c_{pl,\mathrm{av}}$ depends directly on the accuracy of h_f. Thus the measurement of $c_{pl,\mathrm{av}}$ may be refined if a more accurate value of h_f becomes available.

Using Eq. (10) and the Δt intercepts in Fig. 2, the values of the average total hemispherical emissivities at T_m, $\epsilon_{Tm,\mathrm{av}}$, for Zr No. 1 and Zr No. 2 are determined to be 0.30 ± 0.01 and 0.29 ± 0.01, respectively. We have used $\rho_m=5920$ kg/m^3 to compute the sample's surface area A. The density in the isotherm region was approximated by taking the average between the liquid and solid densities at T_m. The liquid and solid densities at T_m were obtained from handbooks (liquid: Ref. 12; solid: Ref. 13). Note that the accuracy of $\epsilon_{Tm,\mathrm{av}}$ depends on the accuracy of h_f and ρ_m, and may be refined as more accurate values become available.

Figure 3 shows the data of Fig. 1 plotted as t vs T^{-3}. Using a best-fit straight line to the plot and Eq. (11), the value of the averaged total hemispherical emissivity of the undercooled liquid, $\epsilon_{Tl,\mathrm{av}}$, for Zr No. 1 is determined to be

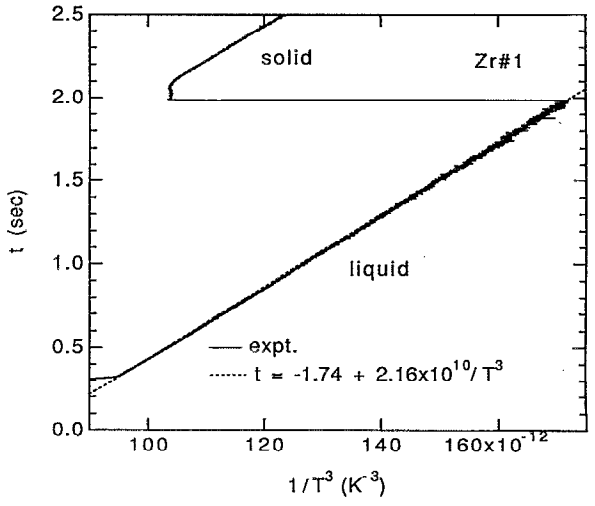

FIG. 3. A typical t vs T^{-3} plot for Zr No. 1 (40.7 mg). A best-fit straight line is superimposed on the experimental data.

0.27 ± 0.01, assuming $\rho_l=5600$ kg/m^3 to compute A.[12] The second sample, Zr No. 2, resulted in 0.28 ± 0.01. The accuracy of $\epsilon_{Tl,\mathrm{av}}$ depends on the accuracy of available values of h_f and ρ_l. There appear to be no published data for the total hemispherical emissivity of zirconium in any form. The spectral emissivities at 650 nm for liquid and solid zirconium are reported to be 0.32 and 0.30, respectively.[12] The measured value of $\epsilon_{Tm,\mathrm{av}}$ may have been affected by a roughening of the surface observed during solidification.

B. Nickel

A typical temperature versus time trace for a 19.4 mg sample of nickel of 99.99% nominal purity (Electronic Space Products, Int'l) is shown in Fig. 4. The pattern of superheating, undercooling, and recalescence is similar to that of zirconium as shown in Fig. 1, except the time re-

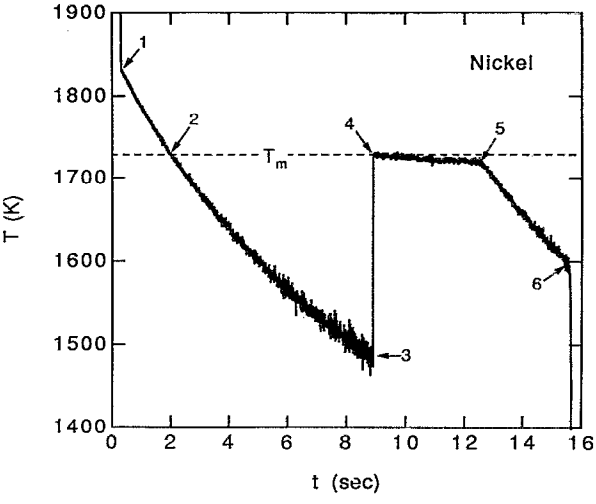

FIG. 4. A typical temperature vs time curve for a 19.4 mg nickel sphere undergoing radiative cooling.

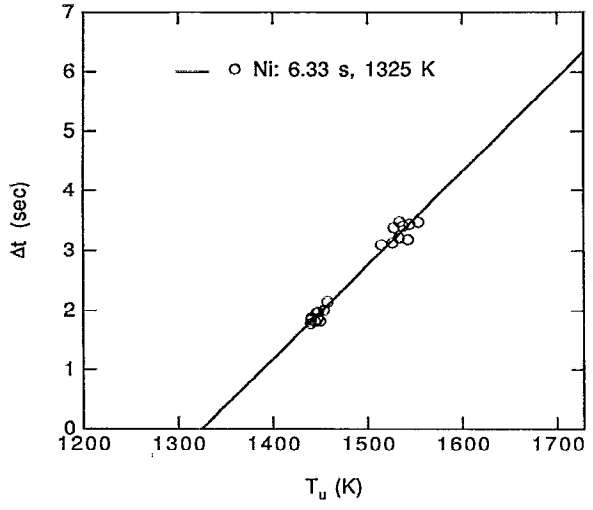

FIG. 5. Δt $(=t_5-t_4)$ vs T_u for the nickel sample (19.4 mg). T_{hyp} and Δt_m are given in the legend.

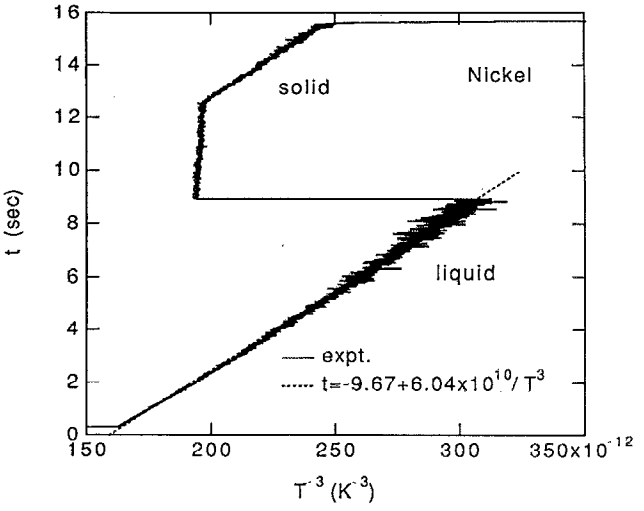

FIG. 6. A typical time vs T^{-3} plot for the nickel sample (19.4 mg). A best-fit straight line is superimposed on the experimental data.

quired to cool the sample is greater because the lower operating temperature led to lower radiative heat fluxes.

As was the case for zirconium, the temperature reading in the post-recalescence isotherm region did not remain exactly constant. For example, in one run it fell 8 K over 3.65 s isotherm duration, which is 0.46% of T_m. For the similar reasons given for zirconium, no corrections have been applied.

Figure 5 shows the Δt vs T_u data. Although the choice of a straight line to fit the data is not as obvious in this case as it was for zirconium, a best-fit straight line has been used to find Δt_m and T_{hyp}. The hypercooling temperature was determined to be 1325 ± 4 K. Using Eq. (8) the value of the average specific heat capacity, $c_{pl,\text{av}}$, of the nickel sample is determined to be 42.6 ± 0.4 J/mol K, assuming $h_f=17.15$ kJ/mol.[14] $c_{pl}(T_m)$ is reported to be 38.49 J/mol K,[14] which is close to the present result for the undercooled liquid. Barth *et al.*[7] found $c_{pl}(T_m)=41\pm2$ and 43 ± 2 J/mol K using drop calorimetry and flux techniques, respectively, which are also close to the present result. We emphasize once again that the accuracy of $c_{pl,\text{av}}$ depends directly on the accuracy of h_f. Thus the measurement of $c_{pl,\text{av}}$ may be refined if a more accurate value of h_f becomes available.

Using Eq. (10) and the Δt intercepts, the value of the average total hemispherical emissivity at T_m, $\epsilon_{Tm,\text{av}}$, for the nickel sample is determined to be 0.21 ± 0.01, assuming $\rho_m=8100$ kg/m^3. The density during the isotherm region, ρ_m, is obtained by averaging the liquid and solid densities at T_m (liquid: Ref. 12; solid: Ref. 15). The accuracy of $\epsilon_{Tm,\text{av}}$ depends on the accuracy of h_f and ρ_m and may be refined in the future.

Figure 6 shows the data of Fig. 4 plotted as t vs T^{-3}. Using a best-fit straight line to the t vs T^{-3} plot and Eq. (11), the value of the averaged total hemispherical emissivity of the undercooled liquid, $\epsilon_{Tl,\text{av}}$, for the nickel sample is determined to be 0.16 ± 0.01, assuming $\rho_l=7900$ kg/m^3 to compute A.[12] The value of $\epsilon_{Tl,\text{av}}$ is significantly less than $\epsilon_{Tm,\text{av}}$. This may be due in part to a roughening of the surface that was observed during solidification. Again, the accuracy of $\epsilon_{l,\text{av}}$ depends on the accuracy of h_f and ρ_l available in the literature.

The total hemispherical emissivity of solid nickel is reported to be 0.12 at 773 K and 0.19 at 1273 K.[12] Extrapolating to T_m, a value of 0.25 is obtained, which is in rough agreement with the present value of $\epsilon_{Tm,\text{av}}=0.21$.

The thermophysical properties of zirconium and nickel are summarized in Table I.

V. DISCUSSION

The present measurement technique is similar to the flux technique of Barth *et al.*,[7] in that both use the post-recalescence isotherm duration to find T_{hyp}, which, in turn, determines the average specific heat of undercooled melts. The present technique, however, is truly containerless, which brings about two main advantages. First, refractory and reactive materials for which no fluxes are

TABLE I. Thermophysical properties of Zr and Ni.

Property material	Zr	Ni
c_{pl} (J/mol K)	40.8±0.9,[a] 40.7[b]	42.6±0.4,[a]39.3,[b]38.5,[c]39.3[f]
$\epsilon_{Tm,\text{av}}$	0.30±0.01[h]	0.21±0.01[h]
$\epsilon_{Tl,\text{av}}$	0.28±0.01[h]	0.16±0.01[h]
T_{hyp} (K)	1769±5[h]	1325±4,[h] 1318±20[i]
$\rho_s(T_m)$ (kg/m^3)	6240[c]	8400[g]
$\rho_l(T_m)$ (kg/m^3)	5600[d]	7900[e]
h_f (kJ/mol)	14.652±0.32[b]	17.15[e]
T_m (K)	2128[d]	1728[d]

[a]Present results, averaged over T_m to T_{hyp}.
[b]Bonnell (Ref. 11) at T_m.
[c]Shaffer (Ref. 13).
[d]Weast and Astle (Ref. 12).
[e]Iida and Guthrie (Ref. 14) at T_m.
[f]Barth *et al.* (Ref. 7), averaged over T_m to T_{hyp}.
[g]Brandes (Ref. 15).
[h]Present results.
[i]Barth *et al.* (Ref. 7).

available can be processed. Second, the cooling process is purely radiative, i.e., it is unaffected by fluxes and gases. Therefore, the total hemispherical emissivities of the undercooled liquid and the solid after recalescence can also be determined.

Metallic and ceramic alloys can be superheated and undercooled as well as pure metals. Phase transformation processes in alloys are more complicated than in pure materials and they depend on the details of their phase diagrams. For example, the post-recalescence temperature of a Ag-Cu eutectic alloy is a function not only of the alloy's composition but of the undercooling temperature.[16] Obtaining the averaged specific heat of the undercooled liquid alloys should still be straightforward utilizing the interception of the Δt-T_u plot with the T_u axis to determine the hypercooling temperature. Obtaining the temperature dependence of the specific heat, however, will require more analysis because of the complexities involved in alloy solidification processes.

We have introduced in this paper a noncontact technique of measuring the specific heat and the total hemispherical emissivity of undercooled states of pure metals. The noncontact approach allowed us to achieve undercooled states of zirconium and nickel which are known to be highly reactive with most crucibles. Furthermore, the noncontact approach allowed us to measure both specific heat and total hemispherical emissivity. The technique introduced in this paper has important implications for the study of solidification processes; in particular, for the selection of various metastable states which have important engineering applications. Studies on more complex materials such as metallic alloys, semiconductors, and glasses are in progress and will be published elsewhere.

ACKNOWLEDGMENTS

We gratefully acknowledge Professor R. Hauge of Rice University for providing us with a preprint of his extensive survey on liquid metal property data. We thank Dr. Eugene Trinh and Dr. K. Ohsaka of the Jet Propulsion Laboratory for valuable discussions and critical comments on the manuscript, Professor F. G. Shi of the University of California, Irvine, for bringing an important paper by Barth *et al.*, to our attention, Mr. Craig Morton of Vanderbilt University for providing the zirconium samples, Mr. Kelly Perry for developing the data analysis software, and Dr. Kin Fung Man, Mr. Daniel Barber, and Mr. Robert McMillan for their generous help throughout the experiments. This work was carried out at the Jet Propulsion Laboratory, California Institute of Technology, under contract with the National Aeronautics and Space Administration.

[1] D. Turnbull, J. Appl. Phys. **21**, 1022 (1950).
[2] E. Schleip, D. M. Herlach, and B. Feuerbacher, Europhys. Lett. **11**, 751 (1990).
[3] R. T. Grimley, Ph.D. thesis, University of Wisconsin, Madison, 1958.
[4] K. Ohsaka, J. R. Gatewood, and E. H. Trinh, Scr. Metall. Mater. **25**, 1459 (1991).
[5] H. S. Chen and D. Turnbull, Acta Metall. **16**, 369 (1968).
[6] J. H. Perepezko and J. S. Paik, J. Non-Cryst. Solids **61&62**, 113 (1984).
[7] M. Barth, F. Joo, B. Wei, and D. M. Herlach, J. Non-Cryst. Solids **156-158**, 398 (1993).
[8] H. J. Fecht and W. L. Johnson, Rev. Sci. Instrum. **62**, 1299 (1991).
[9] W. K. Rhim, S. K. Chung, D. Barber, K. F. Man, G. Gutt, A. Rulison, and R. E. Spjut, Rev. Sci. Instrum. **64**, 2961 (1993).
[10] W. H. Hofmeister, R. J. Bayuzick, and M. B. Robinson, Rev. Sci. Instrum. **61**, 2220 (1990).
[11] Bonnell, Ph.D. thesis, Rice University, 1972.
[12] *CRC Handbook of Chemistry and Physics,* 62nd ed., edited by R. C. Weast and M. J. Astle (CRC, Boca Raton, FL, 1981).
[13] P. T. B. Shaffer, *Plenum Press Handbooks of High Temperature Materials No. 1, Materials Index* (Plenum, New York, 1964).
[14] T. Iida and R. I. L. Guthrie, *The Physical Properties of Liquid Metals* (Clarendon, Oxford, 1988).
[15] *Smithells Metals Reference Book,* 6th ed., edited by E. A. Brandes (Butterworths, London, 1983).
[16] K. Ohsaka and E. H. Trinh, Scr. Metall. Mater. **29**, 845 (1993).